Aust. Met. Mag. 53 (2004) 95-101

The planetary boundary layer, capped by an inversion: extension to baroclinic and stable conditions

G. D. Hess
Bureau of Meteorology Research Centre, Australia

(Manuscript received February 2003; revised October 2003)

In a series of papers Garratt and Hess have shown that advanced models of the neutral, barotropic planetary boundary layer (PBL) overestimate the height of the PBL and underestimate the cross-isobaric angle over land. This leads to other discrepancies between predictions and observations, such as errors in the profile of the longitudinal stress component. Zilitinkevich and Esau attribute these discrepancies to the presence of a capping inversion, however recently Hess has shown that for flow over land the impact of the capping inversion on the PBL structure is small. In this paper sensitivity tests are carried out to assess the possibility that violations of the assumptions of neutral, barotropic conditions may be responsible. It is found that the effects of stable stratification and baroclinicity can both act to improve the agreement between predictions and observations, but for realistic values considering the effects separately, the impact is too small to give complete agreement. The discrepancies are probably due to a combination of violations of the assumptions of steady, horizontally homogeneous, neutral, barotropic flow. Alternatively, the assumption that the eddy viscosity is a scalar may be invalid. A tensor representation of the eddy viscosity would introduce more degrees of freedom, and allow the longitudinal and lateral components of the eddy viscosity to have different vertical profiles.

Introduction

The behaviour of the steady, horizontally homogeneous, neutral, barotropic planetary boundary layer (PBL) has recently been examined by Garratt and Hess. In Garratt and Hess (2002) modelled profiles of the mean wind, the geostrophic departure and turbulent stress components were compared with observations; in Hess and Garratt (2002 a,b) predicted integral measures, such as the geostrophic drag coefficient C_g, the cross-isobaric angle α_0, the parameters A and B of Rossby-number similarity theory, and the rate of dissipation of turbulent kinetic energy integrated over the entire boundary layer, were compared with observations. The parameters A and B are defined as:

$$A = \ln (u_*/|f|z_0) - (kG/u_*) \cos \alpha_0 \qquad ...1$$
$$B = - sign\ (kG/u_*) \sin \alpha_0 \qquad ...2$$

where u_* is the surface friction velocity, f the Coriolis parameter, z_0 the roughness length for momentum, G

Corresponding author address: Dr G.D. Hess, Bureau of Meteorology Research Centre, GPO Box 1289K, Melbourne, Vic. 3001, Australia.
Email: D.Hess@bom.gov.au

the surface geostrophic wind speed (in barotropic flow G is constant with height), k the von Karman constant (k = 0.4), and $sign$ = +1 in the northern hemisphere and –1 in the southern hemisphere. In these studies we found that simple models, e.g., a two-layer analytical model and the mixing-length models of Lettau (1962) and Blackadar (1962, 1965) fit the observations much better than more advanced models, e.g., second-order closure (SOC), large-eddy simulation (LES) or direct numerical simulation (DNS). We attributed this result to two reasons. Firstly, the simple models had (at least) one free parameter that was determined by using atmospheric observations. The more advanced models generally either used more generic methods to determine closure constants, or as in the case of DNS did not have any free parameters. Secondly, the more advanced models are sensitive to the exact nature of the forcing conditions. Although the observations represented near-neutral, near-barotropic conditions, the deviations from the ideal assumptions of the models were significant.

Zilitinkevich and Esau (2002), building on the work of Zilitinkevich and Baklanov (2002) and Zilitinkevich et al. (2002) have suggested that the PBL is often limited by a capping inversion and inclusion of the effects of the inversion would explain the discrepancy between predictions and observations. The introduction of the height of the inversion z_i offers a new vertical height scale which can be used in the similarity equations in place of the Rossby-Montgomery scale $u_*/|f|$. Arya (1975, 1978) argues that h, the actual height of the PBL (this is the same as z_i in our case), is the appropriate length scale for PBL. However, he goes on to say that the scale $u_*/|f|$ is also relevant and there should be an additional similarity parameter h_*, formed by the ratio of the two length scales, $h_* = |f|z_i / u_*$.

Hess (2004) has explored the effect of a capping inversion on PBL structure, and has found that over the sea it can play a significant role. The value of the parameter h_* offers important insight into the dynamics of PBL behaviour. Over the sea where the surface is relatively smooth (z_0 small) mechanical-turbulent forcing is relatively small and the equilibrium boundary-layer height (the height of the capping inversion) is low. Commonly over the sea the inversion height is low enough for $h_* \approx 0.1$, then the longitudinal stress profile becomes nearly linear and the lateral stress profile becomes small. In this case the predictions of the advanced models come into agreement with the observations. However over land the surface is rougher (z_0 large), mechanical-turbulent forcing is relatively large and the equilibrium boundary-layer height is high and $h_* \approx 0.3$, say. Hess found that the impact of the capping inversion was small over land for the steady, horizontally homogeneous, neutral, barotropic case, and that the discrepancies between predictions and observations still exist. Zilitinkevich and Esau (2002) intended their explanation of the role of the capping inversion to apply over land as well as over the sea, but the higher boundary-layer height over land allows the stress vector to rotate with height, and the predictions of the advanced models provide too much mixing over land.

In this paper we explore whether or not it is possible to explain the discrepancies between the predictions and observations by introducing the effects of baroclinicity and stable thermal stratification into the calculations. We will represent the behaviour of the advanced models by a TKE model described in the next section. We then present the predicted profiles of the stress components and compare them with observations from three field experiments conducted over land. This is followed by a summary of our conclusions.

Neutral, baroclinic PBL, capped by an inversion

Many authors have modelled the effects of baroclinicity on the PBL structure (e.g. see Blackadar 1965a,b; Brown 1981; Nieuwstadt 1983; Stubley and Rooney 1986; Brown 1996). In this paper we shall consider a computationally simple model that approximates solutions of second-order closure, LES and other advanced models. The analytical model results of Nieuwstadt (1983) have shown similar behaviour to the model discussed here, and have shown agreement with the second-order closure model of Wyngaard et al. (1974) in barotropic conditions. The present simulations, however, differ from Nieuwstadt's in that we also consider the possible effects of momentum entrainment into the PBL from above, as well as the effects of baroclinicity and stability.

We model the structure of the PBL by employing a turbulent kinetic energy equation model, originally developed by Krishna and Arya (1981) (also see Hess (2004)), and we extend it for stable, baroclinic conditions. In the case of steady, homogeneous flow the equations of motion can be written as:

$$[(U - U_g)/u_*] = sign\ (1/h_*)\ dT_y/d\eta \qquad ...3$$
$$[(V - V_g)/u_*] = -sign\ (1/h_*)\ dT_x/d\eta \qquad ...4$$

where U and V are the components of the mean wind, U_g and V_g the components of the geostrophic wind, and T_x and T_y the non-dimensional components of the stress in surface stress coordinates, and $\eta \equiv z/z_i$ the scaled vertical coordinate. $T_x = -\overline{uw}/u_*^2 = k_* d(U/u_*)/d\eta$ and $T_y = -\overline{vw}/u_*^2 = k_* d(V/u_*)/d\eta$, and $k_* = K_M/(u_* z_i)$ is the non-dimensional eddy viscosity, and $K_M = -\overline{uw}/(dU/dz) = -\overline{vw}/(dV/dz)$ the scalar dimensional eddy viscosity (i.e. the scalar eddy viscosity is only a function of height, not of horizontal direction). This model prescribes a nonlinear eddy viscosity by parametrising the turbulent kinetic energy equation (TKE).

The steady-state TKE equation can be parametrised as:

$$(\tau^2/k_*)(1 - Rf) - (\tau^{3/2}/\lambda_*) + b\, d(\lambda_* \tau^{1/2} d\tau/d\eta)/d\eta = 0 \quad ...5$$

where $\tau \equiv (T_x^2 + T_y^2)^{1/2}$ is the magnitude of the stress. In Eqn 5 the turbulent kinetic energy is assumed to be proportional to τ, i.e. TKE = 1/2 $(\overline{u^2} + \overline{v^2} + \overline{w^2})/ u_*^2 = b\tau$. For flow over a smooth surface wind tunnel measurements indicate the coefficient of proportionality b is given by $b \cong 3$ (Klebanoff 1955; So and Mellor 1972). For aerodynamically rough atmospheric flow and for large Reynolds-number flows in meteorological or environmental wind tunnels the value of b is larger; in these conditions $b \cong 6$ (Counihan 1975; Panofsky and Dutton 1984; Pendergrass and Arya 1984; Arya 2001, p. 209). Based on an average of these observations for large Reynolds-number flows, we have chosen $b = 5.6$, although the stress-profile results shown below are not very sensitive to the value of b.

The first term in Eqn 5 represents the production of TKE due to shearing motions of the mean wind field and buoyancy flux; Rf is the flux Richardson number and is a measure of the stability. For neutral conditions $Rf = 0$; in stable conditions $Rf > 0$. The second term is the parametrised dissipation rate ε nondimensionalised by z_i and u_*, i.e.:

$$(\varepsilon z_i/u_*^3) = (\tau^{3/2}/\lambda_*) \quad ...6$$

where $\lambda_* = k\eta(1 - 0.95\eta)^{1.45}$ is a mixing length determined empirically from wind tunnel data for neutral boundary layer and channel flows. The last term in Eqn 5 is the divergence of the flux of turbulent kinetic energy. The triple moment terms are parametrised using a flux-gradient relationship, where the non-dimensional turbulent exchange coefficient is represented by $\lambda_* \tau^{1/2}$. With these parametrisations Eqn 5 becomes in essence an explicit equation defining the vertical distribution of the eddy viscosity.

For a baroclinic atmosphere the geostrophic wind varies with height. We represent this variation as:

$$U_g/u_* = U_{g0}/u_* + (S_x z_i/u_*)\eta = U_{g0}/u_* + S_{x*}\eta \quad ...7$$
$$V_g/u_* = V_{g0}/u_* + (S_y z_i/u_*)\eta = V_{g0}/u_* + S_{y*}\eta \quad ...8$$

where U_{g0} and V_{g0} are the (constant) surface geostrophic wind components, and S_x and S_y are the (constant) geostrophic wind shear components (in dimensional terms).

From Eqns 3 – 4 and 7 – 8 we obtain the governing equations:

$$d^2T_x/d\eta^2 = -sign\,(h_*/k_*)(T_y - S_{x*}k_*) \quad ...9$$
$$d^2T_y/d\eta^2 = sign\,(h_*/k_*)(T_x - S_{y*}k_*) \quad ...10$$

The coordinate system has the abscissa aligned with the surface stress, which gives the lower boundary conditions for Eqns 3 and 4 as:

$$T_x = 1 \text{ and } T_y = 0 \text{ at } \eta = 0 \quad ...11$$

The upper boundary conditions incorporate the possibility of entrainment of momentum into the PBL from the inversion layer above. These conditions are based on the work of Deardorff (1973). The presence of an inversion immediately above the PBL can cause slip at the top of the PBL and create a discontinuity in momentum, i.e. a velocity jump, there. This discontinuity will cause entrainment of momentum into the PBL to occur. This process can be parametrised by defining an entrainment velocity, W_e, which is multiplied by the velocity jump across the inversion to obtain the momentum flux:

$$\overline{(uw)}_{zi} = -(\Delta U)\, W_e \quad ...12$$
$$\overline{(vw)}_{zi} = -(\Delta V)\, W_e \quad ...13$$

After the velocity jumps are eliminated by using the equations of motion, Eqns 3 and 4, and the definitions of T_x and T_y are inserted, the upper boundary conditions can be written as:

$$T_x = -sign\,(W_{e*}/h_*)dT_y/d\eta$$
$$\text{and } T_y = sign\,(W_{e*}/h_*)dT_x/d\eta \text{ at } \eta = 1 \quad ...14$$

where $W_{e*} = W_e/u_*$. In the results described below W_{e*} is varied from 0 to 10 (this range is wide enough to cover all physically realisable conditions).

We solved Eqns 9 to 11 and 14, using Wippermann's (1971) relaxation method with 1000 iterations at each level and 10 iterations for k_*. The method used is as follows: the initial condition specifies the vertical profiles of the stress components T_x and T_y. Given the values of T_x and T_y, one can determine the value of τ, and then k_* from Eqn 5. New values of T_x and T_y are found at each level of the profile by iteration, alternatively moving upwards through the boundary layer, and then downwards through the boundary layer. After convergence is reached for new values of T_x and T_y, a new value of

k_* is determined from Eqn 5. This process is then repeated until overall convergence is achieved.

The calculations employed 40 equally spaced grid-points in the vertical. The classical Ekman solution for the stress profiles was used as an initial condition:

$$T_x = \exp(-Mz_i\,\eta)\cos(Mz_i\,\eta) \qquad ...15$$
$$T_y = -sign\,\exp(-Mz_i\,\eta)\sin(Mz_i\,\eta) \qquad ...16$$

where $M = 5.0 \times 10^{-4}$ m^{-1}.

The effects of baroclinicity and stability on PBL structure

In Figs 1(a) – 3(a) we show that the TKE model can predict the profiles of the components of the stress for flow over land reasonably well, if it is assumed that the conditions were baroclinic, rather than barotropic. For $h_* = 0.35$ we have included the average neutral, barotropic results for four LES models (Andren et al. 1994) for comparison. The neutral, barotropic results for the TKE model are similar to those of the LES (Hess 2004).

For purposes of illustration we have chosen $h_* = 0.30$, latitude $\varphi = 51.4°$, $u_* = 0.65$ m s^{-1}, $z_0 = 0.14$ m, $z_i = 1711$ m, $S_x = -30\,|f|$ and $S_y = 35\,|f|$ for the Leipzig Experiment (Lettau 1950); $h_* = 0.35$, $\varphi = -34.5°$, $u_* = 0.41$ m s^{-1}, $z_0 = 0.0005$ m, $z_i = 1738$ m, $S_x = -35\,|f|$ and $S_y = -40\,|f|$ for the Pre-Wangara Experiment (Clarke 1970); and $h_* = 0.35$, $\varphi = 51.3°$, $u_* = 0.50$ m s^{-1}, $z_0 = 0.015$ m, $z_i = 1538$ m, $S_x = -25\,|f|$ and $S_y = 15\,|f|$ for the Upavon Experiment (Gill 1967). The actual magnitude of the baroclinicity for these experiments is unknown and the values employed have been chosen in order to achieve approximate agreement between the predicted and observed profiles. For the Leipzig Experiment published estimates vary from $S/|f| \equiv (S_x{}^2 + S_y{}^2)^{1/2}/|f|$ = 0 (Lettau 1957) to 15 (Swinbank 1970). The moderate values of baroclinicity required here to make the predicted profiles agree with observations, while atmospherically possible, seem to be overestimates for experiments in nearly barotropic conditions by factors of at least two or three.

It is noted that the predicted effects of entrainment for these experiments over land for neutral, barotropic conditions are very small (Hess 2004), but when baroclinicity is included the impact of entrainment for the range of W_{e*} considered becomes marked. Baroclinicity (the change of the geostrophic wind with height) affects the wind shear, and thus affects the entrainment velocity. Field programs in which the stress profiles were determined over land for the neutral case have all relied on integrating the geostrophic departure up to the height of vanishing stress. This indirect method of stress determination is used, because over land the diurnal cycle plays such an important role and one cannot anticipate when conditions of prolonged neutral stability are likely to occur with any degree of certainty. Over the sea the diurnal cycle is much less important, and direct measurements of the eddy flux profiles in near-neutral conditions via an aircraft platform have been possible. However, for the range of entrainment values likely to occur (W_{e*} = 0.0 – 0.03) (e.g., see Hess 2004), the predicted entrainment effects are small and affect

Fig. 1 Comparison of the TKE model predictions (solid lines) with observations (circles) of the components of (a) the stress profile for the Leipzig Experimental data (Lettau 1950), assuming neutral, baroclinic conditions (S_x = –30 $|f|$ and S_y = 35 $|f|$); (b) assuming stable, barotropic conditions with the TKE production term reduced by Rf = 0.20 and Rf = 0.65. The TKE model includes different entrainment rates W_{e*} as indicated.

(a)

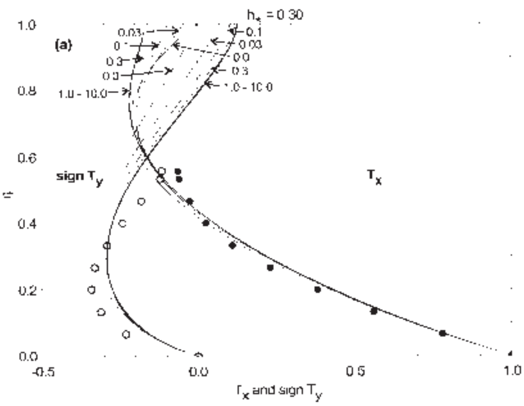

(b)

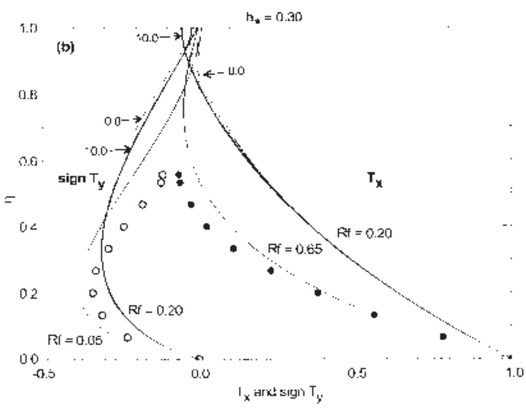

Fig. 2 **Comparison of the TKE model predictions (solid lines) with observations (squares) of the components of (a) the stress profile for the Pre-Wangara Experimental data (Clarke 1970), assuming neutral, baroclinic conditions (S_x = –35 |*f*| and S_y = –40 |*f*|); (b) assuming stable, barotropic conditions with the TKE production term reduced by *Rf* = 0.20 and *Rf* = 0.65. The TKE model includes different entrainment rates W_{e*} as indicated. The dashed lines indicate the results from LES studies for a neutral, barotropic PBL (Andren et al. 1994).**

Fig. 3 **Comparison of the TKE model predictions (solid lines) with observations (triangles) of the components of (a) the stress profile for the Upavon Experimental data (Gill 1967), assuming neutral, baroclinic conditions (S_x = –25 |*f*| and S_y = 15 |*f*|); (b) assuming stable, barotropic conditions with the TKE production term reduced by *Rf* = 0.20 and *Rf* = 0.65. The TKE model includes different entrainment rates W_{e*} as indicated. The dashed lines indicate the results from LES studies for a neutral, barotropic PBL (Andren et al. 1994).**

(a)

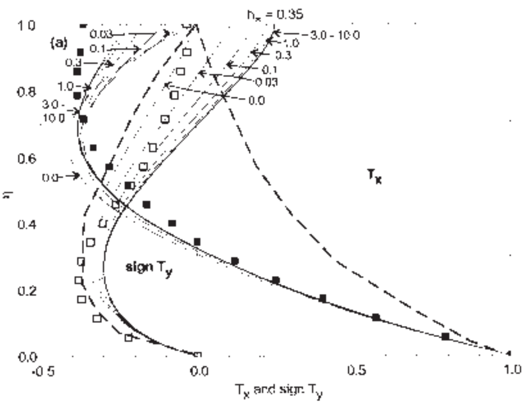

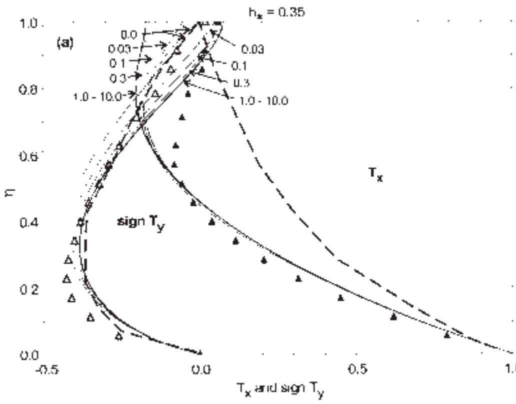

(b)

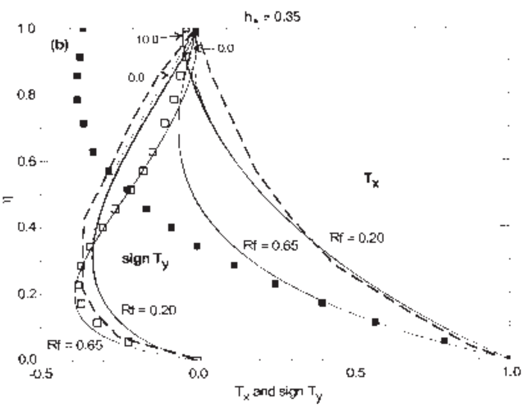

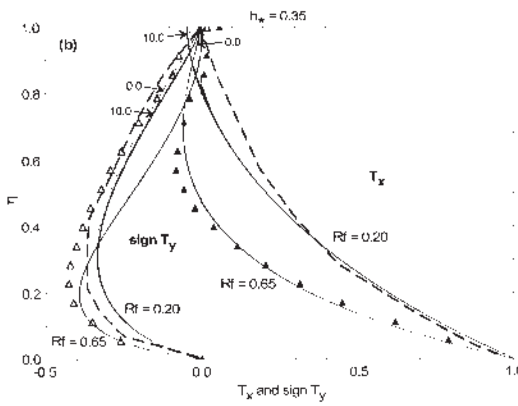

only the upper part of the profiles. The use of the geostrophic departure method, rather than direct measurements, does not explain the discrepancies between the predictions of the advanced models and the observations.

We now consider barotropic flow that is stably stratified. The first term in Eqn 5 represents the production of TKE. In stable conditions $Rf > 0$, the downward flux of heat acts to reduce the production of TKE. Observations indicate that atmospheric turbulence is continuous for $Rf \leq 0.20$ (Beljaars and Holtslag 1991; also see Webster 1964). For the purposes of the present sensitivity tests we assume two extreme values of stability (based on observations): $Rf = 0.20$, the critical value for continuous turbulence, and $Rf = 0.65$, which corresponds to the region of intermittent turbulence (Kondo 1978). Atmospheric measurements of the TKE budget (e.g. Lenschow et al. 1988) show that in stable conditions the contribution of the transport term in the TKE equation is insignificant compared with shear production and dissipation terms, and consequently we neglect the last term in Eqn 5 in the calculations for stable conditions. The resulting profiles are shown in Figs 1(b) – 3(b). The effect of including stable stratification acts to improve the agreement with observations of the longitudinal stress profile (*cf*. Hess 2004). However at the critical *Rf* the stress component profiles differ only slightly from the barotropic profiles. A value of stability well into the intermittent turbulence region is required to make the profiles agree with the observations, and seems to be much too large to be applicable to experiments in nearly neutral conditions.

Concluding remarks

Advanced models of the PBL (TKE, second-order closure, large-eddy simulations, and direct numerical simulations) overestimate the height of the PBL and underestimate the cross-isobaric angle compared with atmospheric measurements for flow over land. This leads to discrepancies between the predicted profile of the longitudinal stress component and observations, as noted by Garratt and Hess (2002); Hess and Garratt (2002 a,b) and Hess (2004). We attribute this disagreement to violations of the strict assumptions of steady, horizontally homogeneous, neutral, barotropic conditions implicit in the observations. Over the sea the diurnal cycle plays only a minor role, but over land it provides significant forcing. Observations of near-neutral conditions may be biased towards stable conditions, and even if they are based on strong winds, they may include the effects of accelerations and/or baroclinic processes.

We have shown that by including the effects of baroclinicity and stable stratification the agreement between the predictions and observations can be improved. However, this demonstration is qualitative only. The original datasets are not comprehensive enough to perform quantitative comparisons. Also we have not investigated the role that accelerations and other factors might play.

We note that the presence of baroclinicity increases the effect of entrainment of momentum from the inversion layer above the PBL; increasing the strength of stable stratification suppresses entrainment in our illustrations.

Our study indicates that baroclinicity may be a more important factor than stability. Including the thermal wind enabled the upper part of the stress profiles to often attain better agreement than merely reducing the TKE production in stable conditions. But in both cases the magnitude of the forcing required to achieve complete agreement seems to be too large for near-neutral, near-barotropic conditions, when the effects are considered separately; the baroclinicity required seems to be too large by a factor of at least two or three and the stability required would be well into the intermittent turbulence regime. The discrepancies between advanced model predictions and observations are probably due to a combination of violations of the assumptions of steady, horizontally homogeneous, neutral, barotropic flow, but we are unable to rule out the alternative explanation that the assumption that the eddy viscosity is a scalar may be invalid. Choosing a tensor representation for the eddy viscosity allows more degrees of freedom, and allows the longitudinal and lateral components of the eddy viscosity to have different vertical profiles. More comprehensive measurement programs are required to better understand the reason for the discrepancies.

Acknowledgments

The author would like to thank Kevin Tory, Jeff Kepert, Dieter Etling and an anonymous reviewer for their comments on an earlier version of the manuscript, and John Garratt, Sergej Zilitinkevich and Pal Arya for stimulating discussions.

References

Andren, A., Brown, A.R., Graf, J., Mason, P.J., Moeng, C.-H., Nieuwstadt, F.T.N. and Schumann, U. 1994. Large-eddy simulation of a neutrally stratified boundary layer: a comparison of four computer codes. *Q. Jl R. Met. Soc., 120*, 1457-84.

Arya, S.P.S. 1974. Comments on "Similarity Theory for the Planetary Boundary Layer of Time-Dependent Height". *J. Atmos. Sci., 32*, 839-40.

Arya, S.P.S. 1978. Comparative effects of stability, baroclinity and the scale-height ratio on drag laws for the atmospheric boundary layer. *J. Atmos. Sci., 35,* 40-6.

Arya, S.P. 2001. *Introduction to Micrometeorology*, Second Edition. Academic Press, San Diego, 450 pp.

Beljaars, A.C.M. and Holtslag, A.A.M. 1991. Flux parameterization over land surfaces for atmospheric models. *Jnl appl. Met., 30*, 327-41.

Blackadar, A.K. 1962. The vertical distribution of wind and turbulent exchange in a neutral atmosphere. *J. geophys. Res., 67*, 3095-102.

Blackadar, A.K. 1965a. A single layer theory of the vertical distribution of wind in a baroclinic neutral atmospheric boundary layer. *Flux of Heat and Momentum in the Planetary Boundary Layer of the Atmosphere, Final Report, AFCRL-65-531*. Department of Meteorology, The Pennsylvania State University, University Park, PA, pp. 1-22.

Blackadar, A.K. 1965b. A simplified two-layer model of the baroclinic neutral atmospheric boundary layer. *Flux of Heat and Momentum in the Planetary Boundary Layer of the Atmosphere, AFCRL-65-531*, Department of Meteorology, The Pennsylvania State University, University Park, 49-65.

Brown, R.A. 1981. Modeling the geostrophic drag coefficient for AIDJEX. *J. geophys. Res, 86*, C3, 1989-94.

Brown, A.R. 1996. Large-eddy simulation and parametrization of the baroclinic boundary-layer. *Q. Jl R. Met. Soc., 122*, 1779-98.

Clarke, R.H. 1970. Observational studies in the atmospheric boundary layer, *Q. Jl R. Met. Soc., 96*, 91-114.

Counihan, J. 1975. Adiabatic atmospheric boundary layers: a review and analysis of data from the period 1880-1972. *Atmos. Environ., 9,* 871-905.

Deardorff, J.W. 1973. An explanation of anomalously large Reynolds stresses within the convective planetary boundary layer. *J. Atmos. Sci., 30*, 1070-6.

Garratt, J.R. and Hess, G.D. 2002. The idealised, neutrally stratified planetary boundary layer. In *Encyclopaedia of Atmospheric Sciences* (J.R. Holton, J. Pyle and J. Curry (eds.)), Academic Press, 1, 267-71.

Gill, A.E. 1967. *The Turbulent Ekman Layer.* Dept. Applied Mathematics and Theoretical Physics, University of Cambridge, UK (unpublished manuscript).

Hess, G.D. 2004. The neutral, barotropic planetary boundary layer, capped by a low-level inversion. *Bound. Lay. Met., 110,* 319-55.

Hess, G.D. and Garratt, J.R. 2002a. Evaluating models of the neutral, barotropic planetary boundary layer: Part I. Overview. *Bound. Lay. Met., 104,* 333-58.

Hess, G.D. and Garratt, J.R. 2002b. Evaluating models of the neutral, barotropic planetary boundary layer: Part II. Modelling observed conditions. *Bound. Lay. Met.., 104*, 359-69.

Klebanoff, P.S. 1955. Characteristics of turbulence in a boundary layer with zero pressure gradient. *NACA Report 1247*. (Also published by Klebanoff in 1954 as *NACA Tech. Note 3178*.)

Kondo, J., Kanechika, O. and Yasuda, N. 1978. Moisture transfers under strong stability in the atmospheric surface layer. *J. Atmos. Sci., 35,* 1012-21.

Krishna, K. and Arya, S.P.S. 1981. Wind structure in neutral, entraining PBL capped by a low-level inversion. *Preprints of the Fifth Symposium on Turbulence, Diffusion and Air Pollution*, 9-13 March 1981, Atlanta, GA, American Meteorological Society, Boston, 65-6.

Lenschow, D.H., Li, X.S., Zhu, C.J. and Stankov, B.B. 1988. The stably stratified boundary layer over the Great Plains. *Bound. Lay. Met., 42*, 95-121.

Lettau, H.H. 1950. A re-examination of the 'Leipzig Wind Profile' considering some relations between wind and turbulence in the frictional layer. *Tellus, 2*, 125-9.

Lettau, H.H. 1957. Winprofil, innere Reibung und Energieumsatz in den unteren 500 m über dem Meer. *Beitr. Phys. Atmos., 30*, 78-96.

Lettau, H.H. 1962. Theoretical wind spirals in the boundary layer of a barotropic atmosphere. *Beitr. Phys. Atmos., 35*, 195-212.

Nieuwstadt, F.T.M. 1983. On the solution of the stationary, baroclinic Ekman-layer equations with a finite boundary-layer height. *Bound. Lay. Met.., 26*, 377-90.

Panofsky, H.A. and Dutton, J.A. 1984. *Atmospheric Turbulence: Models and Methods for Engineering Applications.* John Wiley, New York, 397 pp.

Pendergrass, W. and Arya, S.P.S. 1984. Dispersion in neutral boundary layer over a step change in surface roughness - I. Mean flow and turbulence structure. *Atmos. Environ., 18*, 1267-79.

So, R.M.C. and Mellor, G.L. 1972. An experimental investigation of turbulent boundary layers along curved surfaces. *NASA CR 1940*.

Stubley, G.D. and Rooney, D.R. 1986. Sensitivity of k-epsilon model computation of the neutral planetary boundary layer to baroclinicity. *Bound. Lay. Met., 37,* 53-70.

Swinbank, W.C. 1970. Structure of wind and the shearing stress in the planetary boundary layer. *Arch. Met. Geophys. Bioklim., Ser. A, 19*, 1-12.

Webster, C.A.G. 1964. An experimental study of turbulence in a density stratified shear flow. *J. Fluid Mech., 19*, 221-45.

Wippermann, F. 1971. A note on a method for solving the planetary boundary-layer equations. *Beitr. Phys. Atmos., 44*, 293-6.

Wyngaard, J.C., Coté, O.R. and Rao, K.S. 1974. Modeling the atmospheric boundary layer. *Adv. Geophys., 18A*, 193-211.

Zilitinkevich, S.S. and Esau, I.N. 2002. On integral measures of the neutral, barotropic planetary layer. *Bound. Lay. Met., 104*, 371-9.

Zilitinkevich, S.S. and Baklanov, A. 2002. Calculation of the height of stable boundary layers in practical applications. *Bound. Lay. Met., 105*, 389-409.

Zilitinkevich, S.S., Baklanov, A., Rost, J., Smedman, A.-S., Lykosov, V. and Calanca, P. 2002. Diagnostic and prognostic equations for the depth of the stably stratified Ekman Boundary Layer. *Q. Jl R. Met. Soc., 128*, 25-46.